Solar Energy Materials & Solar Cells 91 (2007) 727–734

www.elsevier.com/locate/solmat

Combination effect of ZnO and activated carbon for solar assisted photocatalytic degradation of Direct Blue 53

N. Sobana, M. Swaminathan*

Department of Chemistry, Annamalai University, Annamalai Nagar 608 002, India

Received 20 August 2006; received in revised form 7 December 2006; accepted 17 December 2006
Available online 7 February 2007

Abstract

The degradation efficiency of AC–ZnO composite photocatalyst was evaluated with solar light using an azo dye Direct blue 53 (DB53) at room temperature. Activity measurements performed under solar radiation have shown good results for the photodegradation of DB53. The synergistic effect observed was ascribed to an extended adsorption of DB53 on activated carbon followed by its transfer to ZnO where it was photocatalytically degraded. The enhanced photocatalytic activity of AC–ZnO when compared to ZnO is found to be due to this synergistic effect. A study on the effects of various parameters like concentration of dye, amount of catalyst and initial pH on the photodegradation of DB53 has been carried out to find optimum conditions.

Keywords: ZnO loaded activated carbon; DB53; Photocatalysis; Synergistic effect; Solar light

1. Introduction

Environmental photochemistry using semiconductors is the part of a general group of chemical remediation methods known as Advanced Oxidation Processes (AOPs). These methods are based on one distinguishing feature—the generation and use of hydroxyl radicals as the primary oxidant for the degradation of organic pollutants. Among the several semiconductors, TiO_2 is reported to be a benchmark photocatalyst [1–4]. However, ZnO is found to be a suitable alternative to TiO_2 [5–8]. For practical applications there are some difficulties such as either filtration of fine TiO_2 or fixation of catalyst particles and efficient utilization of UV/Solar light. For these reasons many researchers have been working to increase the efficiencies of these process by modification of its surface. The design of TiO_2 photocatalyst, anchored or embedded onto support materials with large surface areas that could condense diluted substances would be of great significance, not only to avoid the filtration of small photocatalyst particles, but also to obtain higher efficiency [9,10].

Several authors have proposed a number of modifications on the photocatalysts using a variety of supporting materials and by coating methods [11]. The support materials used are silica, alumina, zeolites, clay and activated carbon. Among these materials, activated carbon is the most commonly used adsorbent for water treatment. Activated carbon has a large specific surface area and a well developed porous structure, resulting in an attractive force toward organic molecules [12–16].

In our earlier work [17,18] we had reported the preparation and characterization of silver doped TiO_2 and four ZnO loaded activated carbon catalysts with 4, 9, 13 and 23% of AC by weight. Among the four ZnO loaded activated carbon catalysts, 9AC–ZnO (9% of AC by weight) has been selected for the degradation study because of its more homogeneous surface, according to the SEM results. In the present work we report the photocatalytic degradation of DB53 with 9AC–ZnO using solar light.

*Corresponding author. Tel.: +91 4144 220572.
E-mail address: chemsam@yahoo.com (M. Swaminathan).

0927-0248/$ - see front matter © 2007 Elsevier B.V. All rights reserved.
doi:10.1016/j.solmat.2006.12.013

2. Experimental

2.1. Materials

ZnO (surface area 5 $m^2 g^{-1}$, particle size 4.80 μm) was obtained from Merck and used as received. Activated carbon from SD fine chemicals (surface area 735.60 $m^2 g^{-1}$, ash content 2.5%, particle size 300 mesh and impurities content of acid solubles 2.5%, water solubles 1.5%) and Direct Blue 53 (DB53), (C.I. No. 23860, molecular formula = $C_{34}H_{24}N_6Na_4O_{14}S_4$, molecular weight = 960.82) from CDH fine Chemicals Company were used as such. Double distilled water was used for all the experiments.

2.2. Preparation of AC–ZnO catalysts

Catalysts with activated carbon were obtained by mixing ZnO and activated carbon at different proportions in an aqueous suspension and this was continuously stirred for 3 h. After this, the mixture was filtered and dried at room temperature. The catalysts have been denoted as *x*AC–ZnO, where '*x*' is the weight percentage of activated carbon (w/w) used in the preparation of the catalyst.

2.3. Catalyst characterization

2.3.1. SEM, XRD and BET surface area measurements

The characterization of the AC–ZnO catalysts using XRD analysis and surface area measurements has been reported [18]. XRD analysis of these catalysts exhibit only patterns assigned to the well crystalline hexagonal phase of ZnO and a small peak at $2\theta = 44.6^\circ$ corresponding to AC. BET surface area measurements indicated that the surface area of the catalysts increases with the increase in the percentage of activated carbon (Table 1). The pore specific volume of AC–ZnO is less when compared to activated carbon, because ZnO particles occupy the pores of activated carbon. The SEM image of 9AC–ZnO (Fig. 1) when compared to the SEM image of AC [18] reveals that the pores of AC particles are occupied by ZnO particles giving a homogeneous coverage. Hence 9AC–ZnO was chosen for the present study.

2.4. Photocatalytic experiments

All photocatalytic experiments were carried out under similar conditions on sunny days of March–April 2004 between 11 AM and 2 PM. An open borosilicate glass tube of 50 ml capacity, 40 cm height and 20 mm diameter was used as a reaction vessel with the total light exposure length of 330 mm. The suspensions were magnetically stirred in the dark for 30 min to attain adsorption–desorption equilibrium between dye and catalyst. Irradiation was carried out in the open-air condition. 50 ml of dye solution with the catalyst was continuously aerated by a pump to provide oxygen and for the complete mixing of reaction solution. During the illumination time no volatility of the solvent was observed.

Table 1
Surface area, crystallite size and pore volume of ZnO, AC and AC–ZnO catalysts

Sample	BET specific surface area ($m^2 g^{-1}$)	Crystallite size (nm)	Pore specific volume ($cm^3 g^{-1}$)
Bare ZnO	5.05	29.70	—
AC–ZnO	75.54	22.70	0.0501
AC	735.60	4.65	0.3730

Fig. 1. SEM image of 9AC–ZnO.

After the attainment of equilibrium in dark, the first sample was taken. After irradiation, 2 ml of the sample was withdrawn for every 10 min and centrifuged to separate the catalyst. 1 ml of the centrifugate was diluted to 10 ml and its absorbances at 603 and 315 nm were measured. The absorbance at 603 nm is due to the color of dye solution and it is used to monitor the decolourisation of dye. The absorbance at 315 nm represents the aromatic content of dye and the decrease of absorbance at 315 nm indicates the degradation of aromatic part of dye. The apparent rate constants for decolourisation and degradation were obtained from the slope of ln (C_0/C) vs. time plot.

UV spectral measurements were done using Hitachi U-2001 spectrophotometer. The pH of the solution is measured by using HANNA Phep (Model H 198107) digital pH meter. Solar light intensity was measured for every 30 min and the average light intensity over the duration of each experiment was calculated. The sensor was always set at the position of maximum intensity. The intensity of solar light was measured using LT Lutron LX-10/A digital Lux meter. The intensity of solar light (1100×100 lux) was nearly constant during the experiments.

3. Results and discussion

3.1. Preliminary experiments

Before studying the various experimental parameters, the photo degradability was tested. When DB53 is exposed to solar light without the catalyst no significant change in concentration of DB53 is observed even after 120 min. This reveals that DB53 does not undergo solar photolysis. DB53 is degraded completely in 240 min in the presence of bare ZnO and solar light whereas AC–ZnO in solar light takes only 120 min to eliminate DB53 from the solution (Fig. 2). Fig. 3 shows the changes in the optical densities at 603 and 315 nm of DB53 degradation by AC–ZnO under different irradiation times.

3.2. Effect of grinding

Before preparing AC–ZnO photocatalyst, AC and ZnO were taken in required ratio and carefully ground in a mortar with the aim of favoring an intimate mixture of both solid phases. The effect of grinding was then followed with respect to (i) DB53 adsorption, (ii) DB53 degradation and decolourisation rates.

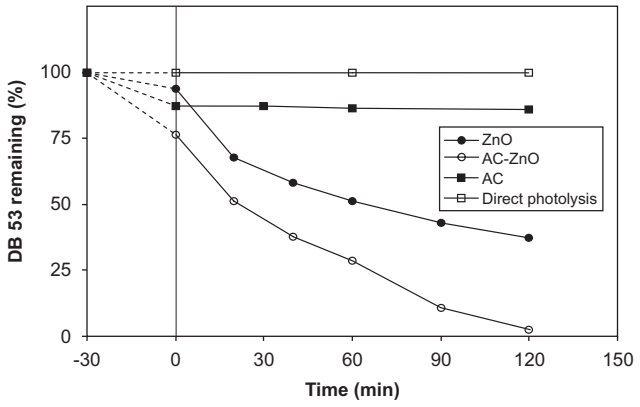

Fig. 2. DB53 degradation in the presence of ZnO, AC–ZnO, AC using solar light, Catalyst = 5 g L^{-1}, [DB53] = 3×10^{-4} mol L^{-1}, pH = 7.0 ± 0.1.

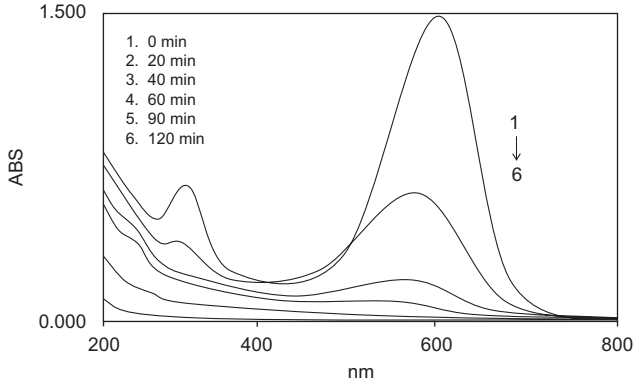

Fig. 3. UV–Visible spectra of DB53 on irradiation in the presence of AC–ZnO AC–ZnO = 5 g L^{-1}, [DB53] = 3×10^{-4} mol L^{-1}, pH = 7.0 ± 0.1.

Grinding had practically negative effect both on adsorption and on the rates of decolourisation and degradation of DB53. The amount of dye adsorbed in dark at 30 min on the ground 9AC–ZnO is less than the dye adsorbed on prepared 9AC–ZnO. Similarly the rates of decolourisation and degradation are also less in ground 9AC–ZnO (Figs. 4a and b). The apparent rate constants of decolourisation and degradation for ground 9AC–ZnO determined from ln (C_0/C) vs. time plot are 4.02×10^{-2}, 2.17×10^{-2} min^{-1}. These values are less than the values 5.19×10^{-2}, 2.49×10^{-2} min^{-1} obtained for prepared 9AC–ZnO.

The grinding of activated carbon and ZnO results in some crystal defects in the ZnO crystal lattice. This affects the crystalline structure of the catalyst. In this process, the increased activity of AC–ZnO catalyst is found to be due to increased adsorption and synergistic effect. If the crystallinity is affected, the adsorption and synergistic effect are reduced. Thus the grinding decreases the photocatalytic activity of the catalyst [19].

3.3. Effect of catalyst loading

The effect of catalyst weight on the decolourisation and degradation of DB53 was investigated by varying the

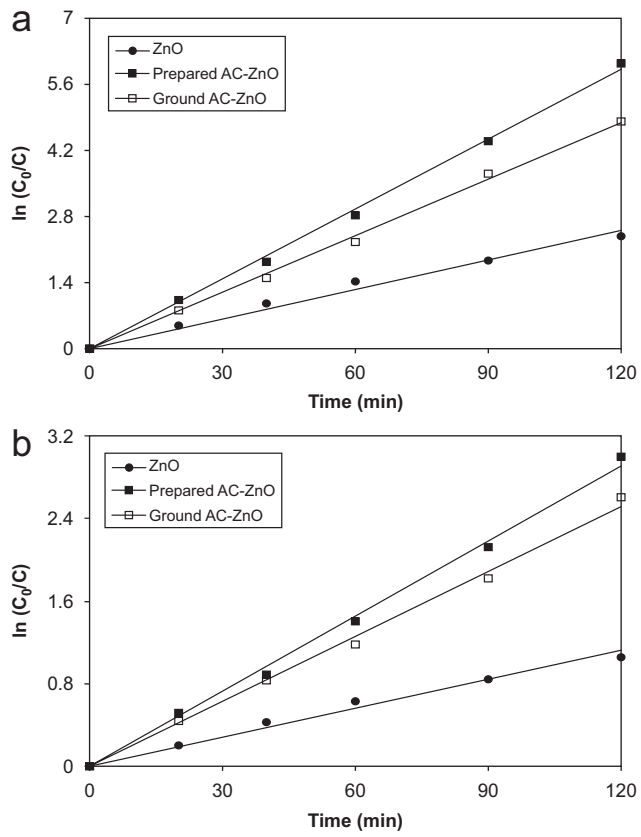

Fig. 4. (a) Kinetics of DB53 degradation for prepared and ground AC–ZnO catalysts using solar light, Catalyst = 5 g L^{-1}, [DB53] = 3×10^{-4} mol L^{-1}, pH = 7.0 ± 0.1 (b) Kinetics of DB53 decolourisation for prepared and ground AC–ZnO catalysts using solar light Catalyst = 5 g L^{-1}, [DB53] = 3×10^{-4} mol L^{-1}, pH = 7.0 ± 0.1.

amount of catalyst from 1 to 6 g L^{-1}. The percentage removal of DB53 with 9AC–ZnO is illustrated in Fig. 5. The results demonstrate that the removal efficiency increases linearly with the catalyst loading upto 5 g L^{-1}. Above 5 g L^{-1} loading of catalyst, the removal efficiency decreases. The enhancement of removal rate is due to (i) the increase in the amount of catalyst weight, which increases the number of dye molecules adsorbed, (ii) the increase in the density of particles in the area of illumination. Above 5 g L^{-1} of catalyst, the removal rate is decreased. This may be due to the enhancement of light reflectance by the catalyst particles and decrease in light penetration [6,7,20,21]. Since the most effective degradation of DB53 was observed with 5 g L^{-1} of 9AC–ZnO, the other experiments were performed using this concentration of 9AC–ZnO.

3.4. Influence of initial pH

The influence of initial pH value from pH 3 to 11 on the percentage removal of DB53 is shown in Fig. 6. It is observed that the removal rate increases with increase in pH up to 9 and then it is almost constant even though the adsorption of dye molecules is low at alkaline pH. From the above fact, it is concluded that the photocatalytic reaction occurs not only on the catalyst surfaces but also in the close vicinity of the catalyst surface. Similar behavior

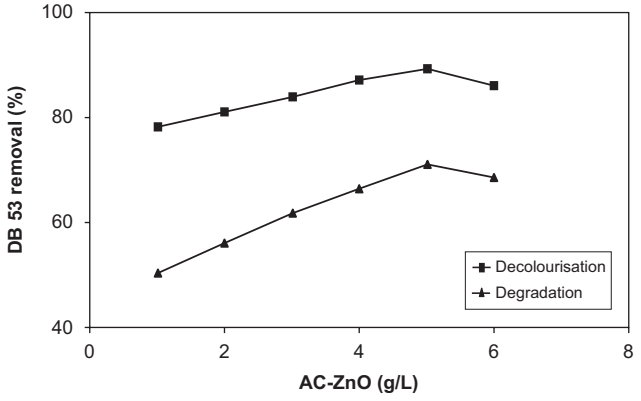

Fig. 5. Effect of catalyst loading on the decolourisation and degradation of DB53 using solar light, [DB53] = 3×10^{-4} mol L^{-1}, pH = 7.0±0.1, irradiation time–decolourisation = 60 min, degradation = 60 min.

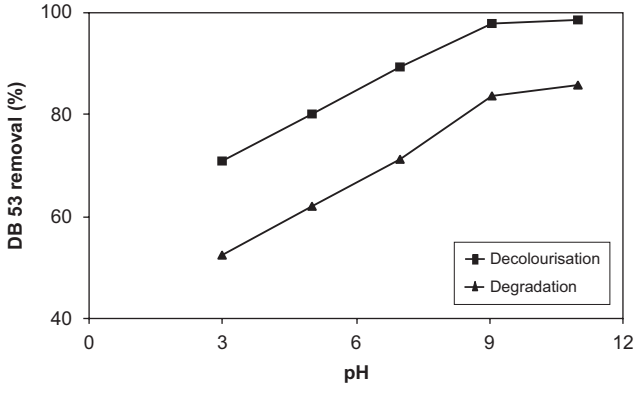

Fig. 6. Effect of initial pH on the decolourisation and degradation of DB53 using solar light, AC–ZnO = 5 g L^{-1}, [DB53] = 3×10^{-4} mol L^{-1}, irradiation time–decolourisation = 60 min, degradation = 60 min.

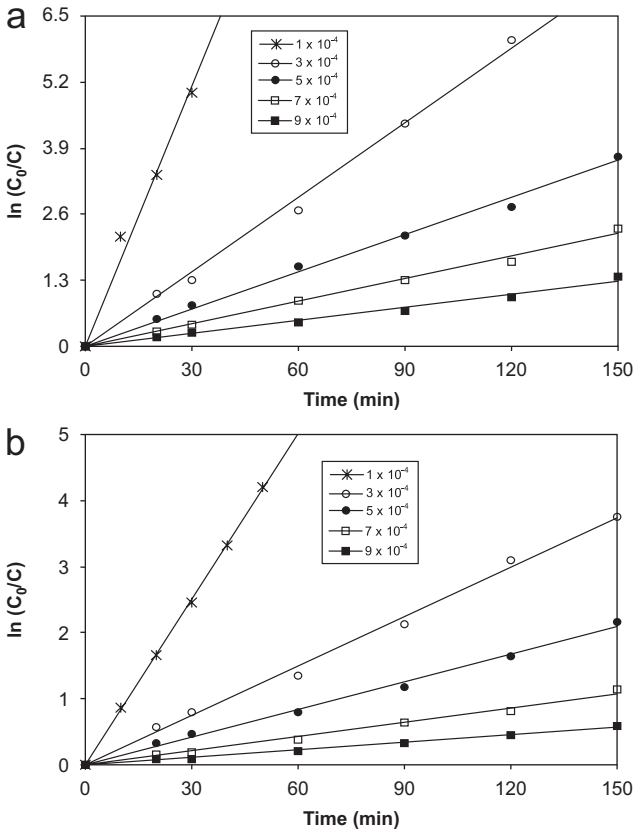

Fig. 7. (a) Kinetics of DB53 decolourisation for different initial concentrations by solar/AC–ZnO AC–ZnO = 5 g L^{-1}, pH = 7.0±0.1 (b) Kinetics of DB53 degradation for different initial concentrations by solar/AC–ZnO AC–ZnO = 5 g L^{-1}, pH = 7.0±0.1.

Table 2
Effect of initial concentration of DB53 on decolourisation and degradation rates

C_0 (10^{-4}) mol L^{-1}	Decolourisation		Degradation	
	k_{app} (10^{-2}) min^{-1}	Time required for 50% decolourisation min	k_{app} (10^{-2}) min^{-1}	Time required for 50% degradation min
1	14.14	4.90	8.35	8.30
3	5.19	13.36	2.49	27.83
5	2.26	30.66	1.37	50.58
7	1.55	44.71	0.70	99.14
9	0.85	81.53	0.35	198.17

k_{app} = apparent rate constant.

was observed in previous studies [22–24]. The acid–base property of the metal oxide surfaces can have considerable implications upon their photocatalytic activity. The point of zero charge for ZnO is 9 and above this value, ZnO surface is negatively charged by means of adsorbed OH^- ions. The presence of large quantities of OH^- ions on the particle surfaces as well as in the reaction medium favors the formation of hydroxyl radical, which is the principal oxidizing species responsible for the dye degradation process. Lizama et al. [25] reported that pH 11 was the optimum value for Reactive Black 19 dye removal. They also commented that textile processes using reactive dyes produced effluents with high pH, suitable for the use of ZnO as a catalyst.

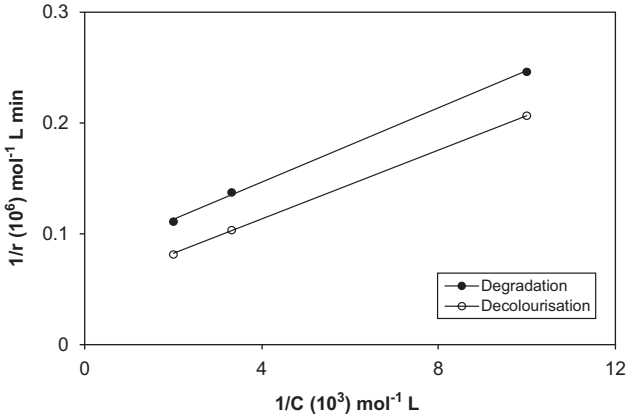

Fig. 8. Linearised reciprocal kinetic plot of the decolourisation and degradation of DB53 by AC/ZnO.

3.5. Effect of initial dye concentration

The effect of pollutant concentration is a very important parameter in wastewater treatment. The effect of initial DB53 concentration was investigated over the concentration range of 1 to 9×10^{-4} mol L^{-1}. The experimental results are presented in Figs. 7a,b and in Table 2 together with time required for 50% degradation for each of the fitted lines.

The results show that the increase in the dye concentration decreases the removal rate and from the Table 2, it is clear that the rate constant k decreases with increase in the initial concentration of DB53. Similar results have been reported for the photocatalytic oxidation of other dyes [26–29]. The initial concentration dependence on the photodegradation rates of DB53 may be due to the following reasons. When the dye concentration increases the amount of dye adsorbed on the catalytic surface increases. This affects the catalytic activity of the photocatalyst. The increase in dye concentration also decreases the path length of photon entering into the dye solution. At high dye concentration the dye molecules may absorb a significant amount of solar light rather than the catalyst and this may also reduce the catalytic efficiency [30].

The influence of initial concentration of DB53 on the photocatalytic degradation rate of most organic compounds is described by *pseudo*-first order kinetics (Eq. (1)).

$$\ln\left[\frac{C_0}{C}\right] = k't, \tag{1}$$

where k' is the *pseudo*-first order rate constant, C_0 is the initial concentration of DB53 and C is the concentration at time 't'.

The experimental data has been rationalised in terms of modified L–H kinetic model to accommodate reaction occurring at solid–liquid interface.

$$r = \frac{K_1 kC}{1 + K_1 C}, \tag{2}$$

$$\frac{1}{r} = \frac{1}{K_1 kC} + \frac{1}{k}, \tag{3}$$

where C is the initial concentration in mg L^{-1}, k is the reaction rate constant and K_1 is taken to be the Langmuir adsorption constant. This Langmuir–Hinshelwood (L–H) kinetic equation has been used by several authors to analyze the heterogeneous photocatalytic reaction [3,31]. The rate of degradation of DB53 at the surface is proportional to the surface coverage of DB53 on the photocatalyst assuming that DB53 is strongly adsorbed on the catalyst surface than the intermediate products [27]. In the L–H equation k reflects the limiting rate of the reaction at maximum coverage under the given experimental conditions and K_1 represents the equilibrium constant for adsorption of DB53 on the illuminated photocatalysts.

At lower concentrations of the dye, Langmuir–Hinshelwood expression has been employed to model the kinetics of heterogeneous photocatalysis of DB53. It was confirmed by plotting the reciprocal of initial rate ($1/r$) against reciprocal of initial concentration ($1/C$) as shown in Fig. 8. The values k and K_1 are found to be 1.96×10^{-5} M min^{-1} and 3.27×10^3 M^{-1} for decolourisation and 1.26×10^{-5} M min^{-1}, 4.72×10^3 M^{-1} for degradation, respectively.

3.6. Synergy effect

The mechanism of semiconductor photocatalysis has been well established. As discussed in literature [16,32] the photocatalytic degradation of organic substrate occurs mainly by the attack of hydroxyl radicals. The addition of activated carbon to ZnO increases the efficiency of degradation.

To simulate the recycling of AC–ZnO catalyst and to confirm the synergistic effect, the prepared AC–ZnO catalyst was repeatedly used. The sample of photocatalyst was kept first in the dark for 30 min to saturate the adsorption of DB53 and then exposed to solar irradiation

(first cycle). After 120 min, the sample was separated from the test solution by filtering and then dispersed again into a virgin solution of DB53 with the same concentration, being again kept in the dark for about 30 min and then irradiated by solar light (second cycle). The plot of percentage of DB53 remaining versus irradiation time for two cycles of photodegradation of DB53 is shown in Fig. 9.There is a slight difference in adsorption on activated carbon between the first and second cycles. This may be due to the higher adsorption of DB53 on a clean surface in the first cycle. But the rates of DB53 removal in both cycles are similar. After 120 min of irradiation, the amounts of DB53 remaining in the first and second cycles are 4.48% and 4.10%, respectively.

This shows that DB53 molecules are initially adsorbed on activated carbon and then diffused to ZnO present in the pores of activated carbon and degraded. From the results of cyclic performance for the degradation of DB53, the reusability of AC–ZnO and synergistic effect are revealed.

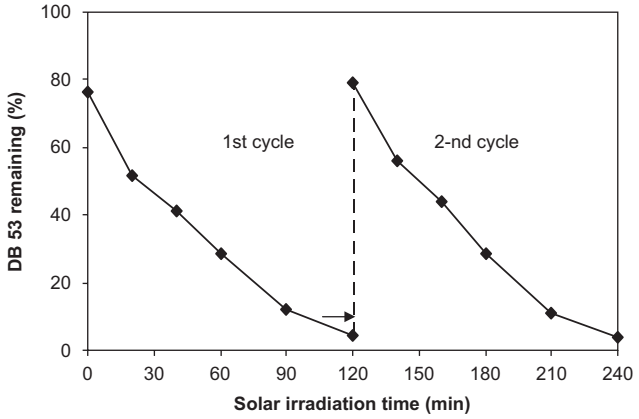

Fig. 9. DB53 degradation during cycles of reuse of AC–ZnO. Arrow represents the transfer of AC–ZnO into fresh DB53 solution.

This synergistic effect is further confirmed by FT-IR studies. The FT-IR spectrum of DB53 dye is given in Fig. 10. Figs. 11a and b give FT-IR spectra of AC–ZnO photocatalyst before and after complete adsorption of dye in dark. FT-IR spectrum in Fig. 11b shows the characteristic peaks of dye DB53 in the region of 1000–1800 cm^{-1}. This indicates the adsorption of DB53 on the AC–ZnO catalyst. The FT-IR spectrum of AC–ZnO photocatalyst after the complete degradation is shown in Fig. 11c. Comparison of Figs. 11b and c reveals that the characteristic peaks of dye on the absorption spectra of AC–ZnO present in Fig. 11b disappeared and the spectrum in Fig. 11c is similar to the spectrum of the catalyst given in Fig. 11a. This reveals that the dye molecules, adsorbed on AC are being transferred to the ZnO present in the pores where they are degraded on irradiation. This synergistic mechanism is shown in Scheme 1. A similar mechanism has been proposed for AC–TiO_2 for the degradation of methylene blue [12].

The synergy factor has been estimated quantitatively using Eq. (4) as reported for AC–TiO_2 [13,19]. The strong synergistic effect of AC–ZnO is shown by the synergy factor of 4.21.

$$R = k_{app}(\text{AC-ZnO})/k_{app}(\text{ZnO}). \quad (4)$$

The synergistic effect for the degradation of DB53 by solar process is very high, because the rate of degradation of DB53 by bare ZnO is very slow and it takes 240 min for complete degradation.

4. Conclusions

Higher photocatalytic activity of ZnO loaded activated carbon for the degradation of DB53 was experimentally proved. It has been shown that the addition of a commercial activated carbon to ZnO under solar irradiation could induce a substantial synergistic effect by a factor of 4.21 in the efficiency of the photocatalyst. It has been

Fig. 10. FT-IR spectra of DB53 adsorbed on KBr.

Fig. 11. FT-IR spectra of (a) fresh AC–ZnO, (b) AC–ZnO after DB53 adsorption and (c) AC–ZnO after complete degradation of DB53.

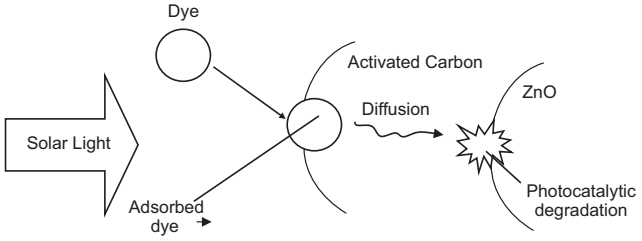

Scheme 1.

explained by adsorption of DB53 on activated carbon and subsequent mass transfer to photoactive ZnO. The degradation follows pseudo first order kinetics. Alkaline pH is found to be better than acidic pH. The grinding of AC–ZnO mixture has a negative effect on the removal of DB53. Obviously, this modified photocatalyst will offer a new possibility in the application of solar photocatalytic reaction to the area of environmental clean up.

References

[1] I.A. Alaton, I.A. Balcioglu, J. Photochem. Photobiol. A: Chem. 141 (2001) 247.
[2] C. Hu, J.C. Yu, Z. Hao, P.K. Wong, Appl. Catal. B: Environ. 42 (2003) 47.
[3] C. Galindo, P. Jacques, A. Kalt, Chemosphere 45 (2001) 997.
[4] G.A. Epling, C. Lin, Chemosphere 46 (2002) 561.
[5] N. Daneshvar, D. Salari, A.R. Khataee, J. Photochem. Photobiol. A: Chem. 162 (2004) 317.
[6] E. Evgenidou, K. Fytianos, I. Poulios, Appl.Catal. B: Environ. 59 (2005) 83.
[7] A. Akyol, H.C. Yatmaz, M. Bayramoglu, Appl. Catal. B: Environ. 54 (2004) 19.
[8] A.A. Khodja, T. Sehili, J.F. Pihichowski, P. Boule, J. Photochem. Photobiol. A: Chem. 141 (2001) 231.

[9] S. Sakthivel, S.U. Geissen, D.W. Bahnemann, V. Murugesan, A. Vogelpohl, J. Photochem. Photobiol. A: Chem. 148 (2002) 283.
[10] A. Dipaola, E. Garicia-Lopez, S. Ikeda, G. Marci, B. Ohtani, L. Palmisano, Catal. Today 75 (2002) 87.
[11] R.L. Pozzo, M.A. Baltanas, A.E. Cassano, Catal. Today 39 (1997) 219.
[12] T. Tsumura, N. Kojitani, I. Izumi, N. Iwashita, M. Toyoda, M. Inagaki, J. Mat. Chem. 12 (5) (2003) 1391.
[13] Y. Xu, W. Zheng, W. Liu, J. Photochem. Photobiol. A: Chem. 122 (1999) 57.
[14] K. Shimizu, T. Kaneko, T. Fujishima, T. Kodama, H. Yosida, Y. Kitayama, Appl. Catal. A: Gen. 225 (2002) 185.
[15] J. Matos, J. Laine, J.M. Herrmann, J. Catal. 200 (2001) 10.
[16] J. Arana, J.M. Dona Rodriguez, C. Garriga i Cabo, O. Gonzalez-Diaz, J.A. Herrera-Melian, J. Perez Pena, G. Colon, J.A. Navio, Appl. Catal. B: Environ. 44 (2003) 161.
[17] N. Sobana, M. Muruganandham, M. Swaminathan, J. Mol. Cat. A: Chem. 258 (2006) 124.
[18] N. Sobana, M. Muruganandham, M. Swaminathan, Catal. Commun. (Communicated).
[19] J. Matos, J. Laine, J.M. Herrmann, Appl. Catal. B: Environ. 18 (1998) 281.
[20] M.S.T. Goncalves, A.M.F. Oliveira-Compos, E.M.M.S. Pinto, P.M.S. Plasencia, M.J.R.P. Queiroz, Chemosphere 39 (1999) 781.
[21] O.E. Kartal, M. Erol, H. Oguz, Chem. Eng. Tech. 24 (2001) 645.16.
[22] S. Sakthivel, B. Neppolian, M.V. Shankar, B. Arabindoo, M. Palanichamy, V. Murugesan, Sol. Ener. Mat. Sol. Cells 77 (2003) 65.
[23] C.A.K. Gouvea, F. Wypych, S.G. Moraes, N. Duran, N. Nagata, P.P. Zamora, Chemosphere 40 (2000) 433.
[24] A. Pandurangan, P. Kamala, S. Uma, M. Palanichamy, V. Murugesan, Indian J. Chem. Technol. 8 (2001) 496.
[25] C. Lizama, J. Freer, J. Baeza, H.D. Mansilla, Catal. Today 76 (2002) 235.
[26] I. Tsachpinis, J. Chem. Technol. Biotechnol. 74 (1999) 349.
[27] I. Poulios, I. Aetopoulou, Environ. Sci. Technol. 20 (1999) 479.
[28] B. Neppolian, H.C. Choi, S. Sakthivel, B. Arabindoo, V. Murugesan, J. Hazard. Mater. B 89 (2002) 303.
[29] N. San, A. Hatipoglu, G. Kocturk, Z. Cinar, J. Photochem. Photobiol. A: Chem. 139 (2001) 225.
[30] A. Mills, R.H. Davis, D. Worsely, Chem. Soc. Rev. 22 (1993) 4 17.25.
[31] F. Chen, Y. Xie, J. He, J. Zhao, J. Photochem. Photobiol. A: Chem. 138 (2001) 139.
[32] J. Arana, J.M. Dona Rodriguez, E. Tello Rendon, C. Garriga i Cabo, O. Gonzalez-Diaz, J.A. Herrera-Melian, J. Perez Pena, G. Colon, J.A. Navio, Appl. Catal. B: Environ. 44 (2003) 153.